ACS OMEGA

Open Access

http://pubs.acs.org/journal/acsodf

Article

Feasibility of Metal Oxide Glasses and Polymer Membranes as Sorbents for Gaseous Oxidized Mercury

Livia Lown, Sarrah M. Dunham-Cheatham,* Paige Murray, Seth N. Lyman, Krista L. Carlson, and Mae Sexauer Gustin

Cite This: *ACS Omega* 2025, 10, 47676−47687

Read Online

ACCESS | Metrics & More | Article Recommendations | Supporting Information

ABSTRACT: Mass spectrometry methods are currently under development by the atmospheric mercury (Hg) research community to elucidate the identity of atmospheric oxidized mercury (Hg^{II}) compounds. Due to high instrument detection limits, materials that can quantitatively preconcentrate atmospheric Hg^{II} without facilitating compound-altering chemical reactions are needed to support these methods. Cation exchange membranes (CEM) and nylon membranes are currently used to preconcentrate ambient Hg^{II} for concentration measurements and Hg^{II} compound estimation, respectively. However, CEM and nylon membranes are poor candidates for observations by mass spectrometry methods due to release of interfering compounds upon heating; glasses do not have this problem. Here, three metal oxide glasses were explored as potential alternatives for Hg^{II} preconcentration for future use with mass spectrometry methods: calcium phosphate (CaP), iron phosphate (FeP), and calcium aluminate (CaAl). The glasses demonstrated quantitative selective capture of $HgBr_2$ without capture of Hg^0. Under ambient conditions, the CaP, FeP, and CaAl sorbed 36.4 ± 12.6% of the total Hg^{II} as the CEM. However, when Hg concentrations were normalized to surface area, CaP, FeP, and CaAl sorbed more $HgBr_2$ in the laboratory and ambient Hg^{II} compared to CEM. The CEM and CaP retained similar concentrations of $HgBr_2$ when preloaded samples were deployed in the field. Additionally, a permeation tube-based calibrator was used to load sorbents with $HgBr_2$ for investigation of Hg^{II} retention on CEM and thermal desorption profile changes on nylon membranes during active sampling. Nylon membranes were purchased from three vendors and used to compare $HgBr_2$ retention; a different $HgBr_2$ thermal desorption profile was achieved for each vendor's nylon membrane.

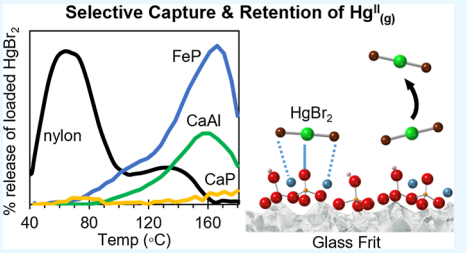

HIGHLIGHTS

- Preconcentration surfaces for oxidized mercury measurements have limitations
- Glasses selectively sorbed Hg^{II}, and sorbed more Hg^{II} per area than CEM under lab and field conditions
- Not all permeated $HgBr_2$ was retained during active sampling
- CEM and CaP retained the most Hg^{II}, and no $HgBr_2$ was released from CaP up to 180 °C
- Differences in membrane manufacturing affects Hg^{II} sorption behavior, efficacy

INTRODUCTION

Mass spectrometry (MS) methods for oxidized mercury (Hg^{II}) compound identification have been tested using laboratory samples at above-ambient concentrations.[1−4] These methods require preconcentration of atmospheric Hg^{II} to provide sufficient Hg^{II} for analysis due to relatively high detection limits. Membranes routinely utilized for atmospheric Hg^{II} preconcentration (e.g., nylon, poly(ether sulfone), polytetrafluoroethylene) are not suitable for direct sample introduction to MS detectors.[5] Thermal desorption (TD) of Hg^{II} from these membranes produces degradation products that interfere with the detection of mercury (Hg) compounds.[2] Observations of compound-altering exchange reactions have been made on both cation exchange membranes (CEM) and nylon membranes at high Hg concentrations.[4] Thus, alternate materials are needed that sorb, retain, and quantitatively release atmospheric Hg^{II} compounds for downstream analysis.

Simple metal oxides tailored to have strong basic sites have shown selectivity for Hg^{II} over Hg^0. Tang et al.[6] evaluated calcium-based sorbents with different constituents and types of basic sites. Calcium acetate monohydrate had stronger basic sites compared to calcium nitrate tetrahydrate and hydrated calcium oxide (CaO), and demonstrated the highest $HgCl_2$ capture of the materials tested. No significant Hg^0 loading was observed for any of the calcium-based sorbents due to minimal acid sites. CaO selectivity for Hg^{II} over Hg^0 was also supported by density functional theory calculations.[6] Other groups have

Received: August 27, 2025
Accepted: September 25, 2025
Published: October 2, 2025

reported sorption of Hg^{II} to aluminum oxide, silicon dioxide, and titanium dioxide based on the acid-base character of the metal oxides.[7−9] Theoretical findings from Tang et al.[10] showed that adsorption energies of $HgCl_2$ increased with oxide basicity in the order of BeO < MgO < CaO < SrO, and Shen et al.[11] identified unsaturated Al and O atoms as active Hg^{II} adsorption sites on Al_2O_3. Strong acidic sites, such as those found on acidic oxides (e.g., SiO_2) or transition metal oxides (e.g., Fe_2O_3), tend to catalytically oxidize gaseous Hg^0 to Hg^{II}.[10,12] Strong basic sites only react weakly (physisorption) with Hg^0, but form strong chemical bonds with Hg^{II}. Therefore, increasing the sorbent surface basicity should increase the selectivity for Hg^{II} over Hg^0. However, how this surface chemistry effects the release of the compounds has yet to be studied in detail. Additionally, there is still little knowledge about the retention of these physiosorbed or weakly chemisorbed species in the presence of atmospheric oxidants and light.

Based on the results from crystalline oxides, we hypothesized that metal oxide glasses would be promising preconcentration surfaces for Hg^{II} compounds. Compared to their crystalline counterparts, that offer well-defined and repeatable active sites, glasses have a continuum of local bonding environments due to their structural disorder. While a lack of well-defined active sites may not be advantageous for precision, compositional and structural flexibility can enhance chemical reactivity to allow for the formation of strongly chemisorbed Hg. The ease of fabrication of glasses into high specific surface area (SSA) geometries would also be advantageous by providing more accessible reactive sites.

In addition to identifying and testing new materials for chemical observations by MS, work is needed to further understand the field performance of CEM and nylon membranes. A recent comparison between two colocated dual channel systems (DCS) and the membrane-based reactive mercury active system (RMAS) demonstrated that DCS Hg^{II} concentration measurements were 30 to 50% higher than CEM measurements when averaged over a 7 to 14 day sampling period.[13] The authors suggested the following as potential explanations for lower CEM measurements compared to DCS measurements: sample loss from CEM during RMAS deployment; Hg^{II} adsorption to RMAS filter pack holders; and/or Hg^{II} generation within the DCS. In a follow up study, Allen et al.[14] showed that Hg^{II} recovered from RMAS filter packs was less than 5% of that captured by membranes, indicating that Hg^{II} sorption to filter packs accounted for only minor differences between RMAS and DCS Hg^{II} measurements. However, sample losses from CEM during deployment have yet to be investigated. Additionally, the original TD method for estimating Hg^{II} compounds, first introduced by Huang et al.[15] and modified by Gustin et al.,[16] has been improved through time (cf., Luippold et al.[17]), but subsequent reported TD profiles of permeated $HgBr_2$ differ in shape,[18] warranting further investigation.

This work investigated the following questions: (1) Can metal oxide glasses be selective for Hg^{II}? Are these sorbents feasible for use as preconcentration surfaces for ambient Hg^{II} (e.g., do they retain Hg^{II} when exposed to atmospheric oxidants and light)? (2) Is Hg^{II}, added as $HgBr_2$ using a custom-built calibrator, retained on materials during active sampling of ambient air? (3) Could differences in TD profiles for $HgBr_2$ through time be due to changes in methods for manufacturing nylon membranes?

METHODS

Materials and Characterizations. Experimental materials for this study included three metal oxide glasses and multiple polymer membranes. Glass compositions were selected to provide a range of surface basicity and chemical reactivity. Reagent-grade chemicals were used to make the glasses: CaP (50 CaO 50 P_2O_5 mol %); FeP (16.4 Li_2O 11.3 K_2O 6.3 Na_2O 26 Fe_2O_3 40 P_2O_5 mol %); and CaAl (64 CaO 36 Al_2O_3 mol %). Alumina crucibles (AdValue Tech, Al-1050) containing 20 g batches were placed into a muffle furnace and heated to the appropriate melting temperature (1200 to 1500 °C) at a rate of 10 °C min^{-1}. After 1 h at temperature, crucibles were removed from the furnace and the melt was poured onto a cooled copper plate. After cooling, the glasses were ground and sieved to a particle size distribution range of 53−106 μm; this material was used for all experiments herein. The CaP[19] and FeP[20] were X-ray amorphous (data not shown). The CaAl composition was determined to be 48.5% crystalline (Figure S1; Text S1). For succinctness, these materials will henceforth be referred to as "glasses", despite the CaAl material being partially crystalline.

CEM are negatively charged, proprietarily treated poly(ether sulfone) membranes (Pall Corporation, 0.8 μm pore size, Mustang-S; P/N MSTGS3R). PTFE (polytetrafluoroethylene, 0.2 μm pore size; P/N 1180747) and nylon (polyamide, 0.2 μm pore size; P/N 2500747N) membranes were purchased from Sartorius Corporation. Nylon membranes from Sterlitech (0.2 μm pore size; P/N NY0247100) and Whatman (0.2 μm pore size; P/N 7402-004) were also utilized to test whether $HgBr_2$ TD profiles differed between manufacturers.

SSA for the metal oxide glasses and CEM was quantified using multipoint Brunauer−Emmett−Teller (BET; Anton Paar Autosorb-iQ), with outgasing at 50 °C for 24 h followed by N_2 adsorption at −196 °C (77 K) or Ar adorption at −186 °C (87 K). Pore distribution size was determined from the argon isotherm using the Barrett−Joyner−Halenda (BJH) desorption pore-size distribution; selected BJH points and pore size distribution plots are shown in Figure S2.

Glass surfaces were examined using X-ray photoelectron spectroscopy (XPS) and scanning electron microscopy/energy dispersive spectroscopy (SEM/EDS; Figure S3). More details on glass surface characterizations are provided in the Supporting Information (Texts S1−S3).

Loading Materials with Hg^0 and Gaseous Hg^{II} in the Laboratory. A summary of all experiments is presented in Table S1. To facilitate loading the materials with Hg, metal oxide glasses were held in borosilicate glass tube traps (traps; 3.97 mm ID, 6.35 mm OD, 51 ± 1 mm length), indented at one end to support a porous PTFE frit (10 to 30 μm pore size, 2.5 mm thickness, Savillex; P/N 730−0065) to secure the material in the tube. Membranes were held in perfluoroalkoxyalkane (PFA) filter packs (Savillex, 47 mm; P/N 403-21-47-22-21-2).

For Hg^0 loading, a target mass of 1.1 ng Hg^0, as calculated with the Dumarey equation,[21] was loaded onto each trap containing 100 ± 5 mg CaP, FeP, or CaAl (n = 8 CaP, n = 9 FeP and CaAl). Hg^0 vapor was drawn from a temperature-stabilized bell jar (20 ± 0.1 °C) using a gastight syringe (Hamilton Company) and injected into the traps through which laboratory air was drawn using a vacuum pump at 0.6 ± 0.3 L min^{-1}. A small mass of activated carbon (30 ± 5 mg), packed in a glass tube downstream of all materials and

https://doi.org/10.1021/acsomega.5c05401
ACS Omega 2025, 10, 47676−47687

separated by an additional PTFE frit to prevent cross-contamination, was used to capture breakthrough Hg^0 (Figure S4).

Gaseous Hg^{II} was loaded onto materials using a custom-built calibrator. The calibrator contained a $HgBr_2$ solid-based permeation tube that was kept under a constant flow of He (12.6 mL min^{-1}) in a temperature-controlled chamber (50 °C). The $HgBr_2$ permeation tube, characterized in Elgiar et al.,[22] was shown to emit gaseous Hg^{II} as $HgBr_2$ using a gas chromatography MS. It was assumed that the gaseous Hg^{II} emitted by the calibrator used in this study was also $HgBr_2$, as the permeation tubes used in both studies were built by the same team following the same protocols (i.e., Elgiar et al.[22] and this study), though there were design differences between the calibrators used in Elgiar et al.[22] (model calib002) and this study (model calib003). The permeation rate of the permeation tube used in this study was reported as 2.2 ± 0.2 pg s^{-1}[23] and 1.8 ± 0.2 pg s^{-1}[24], based on collection on CEM. Data from this work demonstrated the difference in reported permeation rates was a result of permeated Hg^{II} loss to the PFA filter pack when gaseous Hg^{II} was loaded at the filter pack inlet (5.5 cm from membrane)[25] versus 2 cm from the membrane.[23] These data and experimental procedure are available in the Supporting Information (Text S4 and Figures S5, S6).

To determine quantitative gaseous Hg^{II} sorption potential in the laboratory, CaP, FeP, and CaAl were exposed to gaseous Hg^{II} as $HgBr_2$ from the calibrator in laboratory air (n = 9 each). The mass of Hg recovered from each material was then compared to the mass of Hg recovered from concurrently exposed CEM. Additional CEM were used downstream of each sample to capture breakthrough Hg^{II}. To observe retention and chemical changes at masses comparable to previous permeation work while maintaining precise loadings with the calibrator, CEM, CaP, FeP, and CaAl were loaded with a target mass of 1 ng Hg^{II} (as $HgBr_2$) from the calibrator, and nylon membranes were loaded with 0.2 ng Hg^{II} (as $HgBr_2$).[15,18] A mass of 0.2 ng Hg on nylon membranes corresponds to a reported concentration of ∼18 to 22 pg Hg m^{-3} and is within the range of observed atmospheric Hg^{II} loadings for one-week deployments in the RMAS (cf. Gustin et al.[26]).

Triplicate method blanks of each material per experiment were exposed to laboratory air without the Hg vapor injection and analyzed concurrently with the Hg-loaded materials to blank-correct measurements. Hg recoveries from method blanks were below the detection limit or low compared to the mass of Hg loaded on the materials (Table S2).

Loading Materials with Ambient Hg^{II} in the Field. RMAS manifolds (cf., Luippold et al.[26]) were used in field deployments to load materials with ambient Hg in the field. The RMAS consisted of an aluminum shield that supported six sampling lines. Each sampling line contained a 1 L min^{-1} critical flow orifice (Teledyne API; P/N 941100) to standardize the flow rate through each line and was attached to a vacuum pump. Triplicate 1 wk deployments were conducted at the University of Nevada, Reno College of Agriculture, Biotechnology & Natural Resources Agricultural Experiment Station Valley Road Greenhouse Complex (39.5375, −119.8047, 1370 masl). This site is impacted by vehicle emissions due to the proximity of Interstate 80 (<100 m distance from active samplers) and long-range transport of pollutants.[26,27] The standard flow through each filter pack and trap was measured (BGI tetraCal) at the beginning and end of each deployment. The mean of beginning and end flow rates was used to calculate the Hg^{II} concentration (pg Hg m^{-3}) in ambient air sampled on each material (n = 3 per material per deployment). Based on comparisons of previous measurements between sensors located directly adjacent to samples in the RMAS manifold and sensors deployed ∼120 m away in an open field during all seasons, the RMAS manifold does not affect the local sampling environment;[28] thus, it was assumed that the samples in this study experienced ambient temperature and relative humidity conditions.

$HgBr_2$ Retention on Materials during Active Ambient Air Sampling. To test metal oxide glasses for gaseous Hg^{II} retention during field deployment, triplicate traps containing CaP, FeP, or CaAl were codeployed with CEM in the field for 1 week. Hg^{II} recovered from these surfaces at the end of deployment was compared to Hg^{II} recovery from codeployed CEM to determine the potential for these materials to be used as preconcentration surfaces for Hg^{II} quantification under field conditions. Additionally, triplicate traps of each glass and CEM were loaded with $HgBr_2$ then codeployed to quantify Hg^{II} losses during active sampling of ambient air. Triplicate deployments were performed (June, July, and August). Materials were stored following the same procedure as above.

To test CEM for gaseous Hg^{II} retention during field deployment, replicate (n = 9 per deployment) CEM were loaded with $HgBr_2$ in laboratory air before deployment in the RMAS ("pre-deployment"). Three of these CEM were immediately frozen at −20 °C ("laboratory controls") to determine the mass of $HgBr_2$ loaded onto deployed membranes, and the remaining six CEM were deployed in the RMAS sampling ambient air for 1 week. Of these six CEM, three were deployed with an upstream PTFE and three without. PTFE were used to compare results when gaseous Hg^{II} (loaded as $HgBr_2$ on CEM deployed downstream of PTFE) was separated from ambient particulate-bound Hg^{II} (captured on upstream PTFE) versus when both gaseous Hg^{II} (loaded as $HgBr_2$) and ambient particulate-bound Hg^{II} were on the same membrane (loaded CEM without an upstream PTFE). Six nonloaded CEM (three with an upstream PTFE, three without) were codeployed in the RMAS to measure ambient Hg^{II} ("field controls"). An additional six CEM were concurrently deployed (three with an upstream PTFE, three without) that were loaded with $HgBr_2$ after the deployment ("post-deployment"). A second set of laboratory controls were taken at the end of deployment with the postdeployment membranes. All CEM were deployed with a second downstream CEM to quantify breakthrough, following standard RMAS procedures.[17] Nylon membranes were loaded and codeployed with CEM in the same manner, with the same replication, then analyzed by TD (described below). All materials were immediately frozen at −20 °C upon collection, pending analysis; potential $HgBr_2$ losses during storage are discussed below. Six deployments were performed in total, three during the winter/spring (February and March, denoted as spring from herein) and three during the summer (June and August), to assess potential seasonal effects on retention of gaseous Hg^{II}.

Environmental conditions (e.g., air temperature, relative humidity, precipitation) for each deployment are provided in Table S3. Materials were analyzed following the quantification methods below.

https://doi.org/10.1021/acsomega.5c05401
ACS Omega 2025, 10, 47676−47687

Percent recovery of loaded $HgBr_2$ was calculated for each material by dividing the Hg concentration (pg Hg m^{-3}) recovered from the loaded material by the sum of the average Hg concentration on the laboratory control (average pg Hg loaded on the material divided by the average volume of ambient air drawn through the material in the field) and the average Hg concentration recovered on the field controls, then multiplied by 100. Per deployment, % recovery was calculated for each loaded material, including both pre- and postloaded. To calculate % recovery from CEM that were deployed downstream of a PTFE membrane, the mass of Hg recovered from the upstream PTFE membrane was added to the mass of Hg recovered from the CEM; this was true for both the loaded material and field control terms.

Percent breakthrough of loaded $HgBr_2$ from materials was calculated for each material by dividing the Hg concentration (pg Hg m^{-3}) recovered from the downstream CEM by the sum of the Hg concentrations recovered from the upstream material and the downstream CEM, then multiplied by 100. Blank-corrected pg Hg m^{-3} recoveries were used for this calculation.[26]

Hg^0 and Hg^{II} Quantification. Hg^0 sorbed to CaP, FeP, CaAl, and activated carbon was quantified by EPA Method 7473 using a Nippon MA-3000 direct Hg analyzer (detection limit = 0.1 ng). The analyzer was calibrated ($r^2 > 0.999$) using a liquid standard (Inorganic Ventures; P/N MSHG-1PPM). At the beginning of each analytical batch, instrument performance was verified with National Institute of Standards and Technology certified reference material 1547. This standard was analyzed again every ten or fewer samples to verify ongoing instrument performance. Recovery within ±10% of the certified value and RSD <5% were considered acceptable for analysis validation.

Hg^{II} captured on CEM, CaP, FeP, and CaAl was recovered using a modified version of EPA Method 1631, following Lown et al.[24] Briefly, each sample was suspended in 1% HCl solution, then digested overnight with BrCl. Excess BrCl was quenched using 30% $NH_2OH{\cdot}HCl$. Hg in an aliquot of the digestate was then reduced with $SnCl_2$ and quantified by cold vapor atomic fluorescence spectroscopy using a Tekran 2600-IVS system that had been calibrated across the analytical range ($r^2 > 0.999$). Ongoing precision recovery check standards (Inorganic Ventures; P/N MSHG-1PPM) were analyzed every ten samples or fewer. Per EPA Method 1631, recovery of check standards within ±15% of the expected value was considered acceptable for analysis. Reagents were purchased from Fisher Scientific and included Optima HCl (P/N A466-500), KBr (P/N P205-500), $NH_2OH{\cdot}HCl$ (P/N H330-500), and $SnCl_2$ (P/N T142-500). $KBrO_3$ was purchased from Acros Organics (P/N 268392500).

Additionally, Hg^{II} retention on $HgBr_2$-loaded CaP, FeP, and CaAl was investigated using a custom-built programmed TD oven coupled to a downstream Tekran 2537 analyzer; this thermal desorption setup has been previously reported in detail.[17] The temperature was ramped from 45 to 180 °C (2 °C min^{-1}), and thermally released Hg was pulled downstream in Hg-free air through a thermolyzer (to reduce any Hg^{II} to Hg^0 for quantitative capture) and into the analyzer for quantification. The reported temperatures are the temperature the sample experienced during the TD analysis, as measured by replicate ($n = 12$) oven calibrations. Triplicate samples of each material were tested.

Thermogravimetric analysis with simultaneous mass spectrometry (TGA-MS; Pfeiffer GSD 350 Omnistar) was also performed on ∼100 mg aliquots of the glass samples before and after exposure to $HgBr_2$, and on glass samples exposed to high humidity (80% relative humidity for 5 h) to evaluate the release of other species (e.g., H_2O, Br_2) from the glass surfaces up to 400 °C.

$HgBr_2$ Chemistry on Nylon Membranes. The TD profile of $HgBr_2$ loaded onto Sartorius brand nylon membranes was tested under three experimental conditions. First, to determine if the TD profile of permeated $HgBr_2$ changed during active sampling of ambient air, nylon membranes were loaded and deployed in the RMAS during the Hg^{II} retention experiments, as described above for CEM. TD profiles of pre- and postdeployment laboratory controls and nonloaded field controls were compared to membranes that were loaded pre- or postdeployment; this comparison was made for membranes deployed with and without upstream PTFE. Second, to understand if the TD profile of membranes loaded with $HgBr_2$ in laboratory air changes during storage, indicating chemical reactions on nylon membranes over time, nylon membranes ($n = 12$ per set) were loaded with 0.2 ng Hg (as $HgBr_2$) and were either immediately analyzed or stored at −20 °C then desorbed 3, 7, or 14 days after loading ($n = 3$ per condition, or 12 per set); triplicate sets were tested. Third, TD profiles for $HgBr_2$-loaded nylon membranes were generated using Sartorius, Sterlitech, and Whatman brand membranes to determine if differences in manufacturing could result in differences in TD profiles. In addition, nylon membranes manufactured by Sartorius, but sold by different vendors (i.e., Sartorius and Cole-Parmer) that were produced within 4 months of each other were subjected to the same loading, deployment, and analysis methods as described above. All nylon membranes were thermally desorbed using the method described in Luippold et al.[17]

Fourier transform infrared spectroscopy (FTIR; Thermo Scientific Nicolet iN10MX Infrared Microscope with Ge attenuated total reflectance crystal) was used to probe for structural differences between nylon membranes from different manufacturers. Each material was scanned from 400 to 4000 cm^{-1} with a resolution of 4 cm^{-1} ($n = 10$ scans per nylon material).

Data Processing and Statistical Analyses. Because the metal oxide glasses and membranes had different SSA, measured Hg concentrations were normalized to better compare Hg sorption behavior on a surface area basis. The SSA-normalized data must be interpreted with caution, as only a small amount of metal oxide was used; thus, the total surface area of metal oxide used in each experiment (0.14 ± 0.01 m^2) was small relative to the total surface area of CEM used (2.85 m^2).

One-way ANOVA and Tukey's honestly significant difference tests were performed in R (R Core Team, 2023, version 4.3.1). Excel 2016 was used to perform Student's t tests and to calculate means (μ) and standard deviations (σ) that are presented as $\mu \pm 1\sigma$. A Grubb's test was also performed in Excel to exclude an anomalously high recovery from CaP during Hg^0 sorption tests. Statistical significance was determined at $\alpha \leq 0.05$ for all tests. Reduced major axis (RMA) regression was used for determining differences in slopes between different TD data sets, as the x-axis measurements had their own associated error. For all RMA analyses, the TD profiles were divided into 2 regions: 40 to

https://doi.org/10.1021/acsomega.5c05401
ACS Omega 2025, 10, 47676−47687

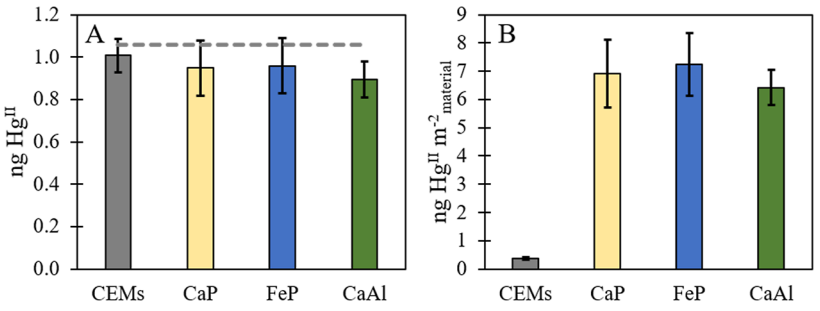

Figure 1. Comparison of (A) mass of Hg^{II} recovered from $HgBr_2$ permeated on metal oxides and CEM, and (B) the same data normalized to material surface area, when permeated in laboratory air. Horizontal bar indicates the calculated Hg^{II} exposure, representing 100% recovery. Error bars indicate 1σ (n = 8 to 9).

110 °C and 115 to 165 °C, based on the bimodal profiles of $HgBr_2$ controls. RMA analyses were performed using the lmodel2 package in R.[29]

RESULTS AND DISCUSSION

Glass Structure. As the goal of this study was to test the feasibility of glasses to selectively capture and retain Hg^{II}, the structure, and hence, resulting surface properties, were inferred from previous studies. For CaP and FeP, the P_2O_5 acts as the network former (PO_4^{3-} units).[30] Phosphate tetrahedra in glasses exhibit resonance hybridization, where the P−O bonds are delocalized and have partial double-bond character. This terminal nonbridging oxygen in each tetrahedron favors the formation of chain- and ring-type structures over three-dimensional connected networks, contributing to structural flexibility and chemical reactivity. Structures are described by Q^n groups, with Q and n representing the structure of the PO_4 tetrahedral units and number of bridging oxygens, respectively. For CaP, Ca^{2+} acts primarily as a network modifier, leading to the formation of a phosphate glass network dominated by metaphosphate (Q^2) units.[30] This moderate degree of network connectivity, coupled with the high basicity of Ca−O sites associated with nonbridging oxygen, is likely responsible for stronger interactions with Hg^{2+}. In contrast, the FeP composition includes multiple alkali ions functioning as network modifiers, while Fe^{3+} can act as both a modifier and a partial network former depending on its local environment.[31] The high alkali content would typically result in a high fraction of nonbridging oxygen species and a less connected network. However, as previous studies have shown, Fe/P ratios above ∼0.4 increase the number of Fe^{3+} species and provide bridging oxygens in Fe−O−P or Fe−O−Fe linkages.[32,33] Consequently, the surface basicity of FeP is likely lower than that of CaP, despite its higher oxygen content, due to a reduction in basic nonbridging oxygens. Future studies explicitly evaluating surface basicity and acidity are needed to substantiate these mechanistic interpretations.

The CaAl composition was determined to be 48.5% crystalline (Figure S5). In the glass, the Ca^{2+} acts as the network modifier in an Al_2O_3 network (AlO^{4-} units).[34] The crystalline phases consisted primarily of mayenite ($Ca_{12}Al_{14}O_{33}$; PDF Card no.: 01-070-2144), with minor calcium aluminate phases, including $CaAl_2O_4$ (PDF Card no.: 01-080-3836) and $Ca(AlO_2)_2$ (PDF Card no.: 00-001-0888) (Figure S7). Formation of these crystalline phases depletes the melt of both Ca and Al, but in proportions that result in a residual glassy phase enriched in CaO relative to the original batched composition. This CaO enrichment increases the fraction of nonbridging oxygens and reduces network connectivity, producing a more modifier-rich and basic glassy matrix surrounding the crystalline phases. The presence of the crystalline phase could lead to more low-coordinated oxygen. For all glasses, the surfaces are expected to be hydroxylated, limiting the ability of the high electron-density surface states (i.e., O-based sites) to act as nucleophiles.

Hg^{II} Selectivity of Metal Oxides under Laboratory Conditions. No quantifiable Hg was recovered from metal oxide glasses loaded with Hg^0 under laboratory conditions. The target mass of 1.1 ng Hg was recovered entirely as breakthrough on the downstream activated carbon (1.1 ± 0.1, 1.2 ± 0.2, and 1.2 ± 0.2 ng Hg for CaP, FeP, and CaAl, respectively).

A mass range of 0.95−1.16 ng Hg^{II} (loaded as $HgBr_2$) was permeated onto and recovered from the glasses (1.01 ± 0.08 ng Hg^{II} with 0% breakthrough on CEM, 0.95 ± 0.13 ng Hg^{II} with 0% breakthrough on CaP, 0.96 ± 0.13 ng Hg^{II} with 0.3 ± 0.8% breakthrough from FeP, and 0.89 ± 0.08 ng Hg^{II} with 0.5 ± 1.4% breakthrough from CaAl) (Figure 1A). The % recoveries of loaded $HgBr_2$ from the glasses were not statistically different from CEM (ANOVA). The resulting type II isotherms (data not shown) for the metal oxides from N_2 physisorption experiments indicated they were either nonporous or macroporous, with little-to-no hysteresis between the adsorption and desorption curves. The CEM isotherm showed no steep uptake at low p/p_o and no type I profile, indicating an absence of significant micropore volume. The metal oxides had a BET SSA of 1.41 $m^2\ g^{-1}$ and the CEM had a BET SSA of 35.17 $m^2\ g^{-1}$. Pore size distrubtion from the BJH on the CEM indicated the pore network was dominated by mesopores >2 nm (Figure S2). When the recoveries were normalized by the material SSA, the capture efficacies of the metal oxides were greater than the CEM capture efficacy (Figure 1B). Caution should be used when drawing conclusions from the normalized results, however, as the CEM material has over an order of magnitude more surface area per mass of material, effectively lowering the normalized CEM results relative to the metal oxides results. The sorption capacity of each material was not determined, though the CEM is not close to Hg saturation with the experimental 1 ng of loaded Hg^{II}.[18] Together, these results indicate that the glasses are capable of selective sorption and capture of a large Hg^{II} loading on a small amount of material surface area in laboratory air. Hg^{II} selectivity results for nylon membranes are available in the Supporting Information (Text S5).

Retention of $HgBr_2$ on Membranes and Metal Oxides When Actively Sampling Ambient Air. Ambient Hg^{II}

https://doi.org/10.1021/acsomega.5c05401
ACS Omega 2025, 10, 47676−47687

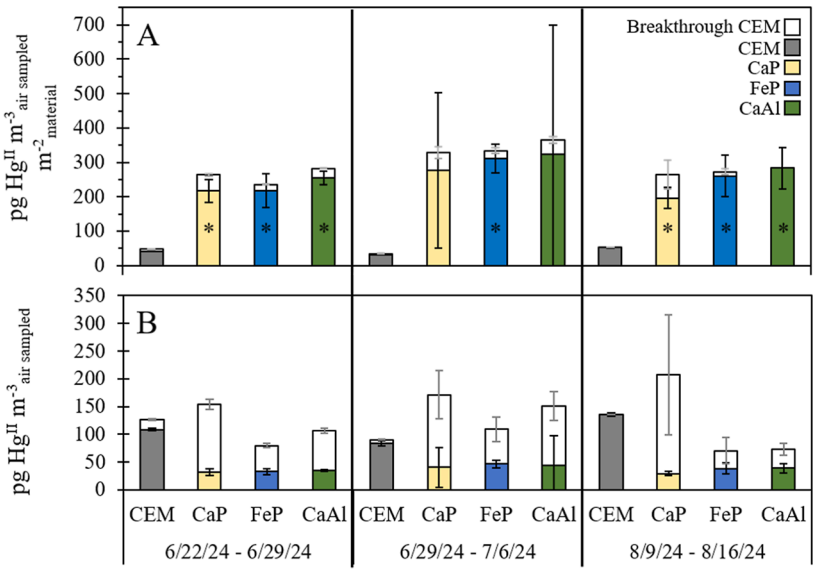

Figure 2. Comparison of ambient Hg^{II} collected on CEM relative to the metal oxide materials, as well as breakthrough, for triplicate RMAS field tests. Error bars indicate 1σ (n = 3); black error bars are for the materials, and gray error bars are for breakthrough. * indicates statistical significance relative to the CEM (α = 0.05), and applies to both A and B panels.

concentrations measured on metal oxide glasses after field deployment were lower than that measured on CEM (Figure 2B). The metal oxide materials also had significantly more breakthrough than CEM. When normalized to SSA, CEM Hg^{II} concentrations were lower than for glasses per m^2 of material deployed. Hg^{II} concentrations measured from the glasses were consistent, with the greatest breakthrough measured for CaP (Figure 2). The metal oxides worked well under laboratory conditions; however, the lower concentrations on metal oxides indicated a lack of retention in the field and suggest that some air constituents could be competing with the Hg^{II} for adsorption with active sites, interfering with Hg^{II} collection and/or promoting Hg reduction. The compositions and structures of these glasses that lead to higher basicity may also increase surface hydration and weathering (i.e., glass surface durability in humidity). However, samples exposed to 80% humidity displayed no evidence of weathering, with no notable mass loss observed by TGA. Regardless, as shown in Figure 2A, the per-surface-area performance of the glasses was superior to that of CEM, suggesting promise for future engineered forms with increased surface area.

For the six field campaigns with membranes loaded with $HgBr_2$ prior to deployment (with and without upstream PTFE), 90 ± 12% (Figure S8) and 75 ± 18% $HgBr_2$ was retained on the CEM and nylon membranes, respectively. No significant Hg^{II} loss occurred from CEM and nylon membranes loaded with $HgBr_2$ after the field deployment (106 ± 10% and 107 ± 14% recovery, respectively). These results indicated that ~10% of loaded $HgBr_2$ was lost from CEM during 1 wk of active sampling of ambient air. Hg^{II} retention was not significantly different in the spring versus summer (n = 18, t-test). CEM Hg^{II} concentrations from loaded $HgBr_2$ on CEM downstream of PTFE membranes were not statistically different from those without (data not shown, n = 36 per condition, t-test), similar to previous studies.[25,27] Nylon results are discussed in more detail in the next section.

CEM laboratory controls taken during field deployments showed complete retention of the loaded $HgBr_2$ from CEM when stored for up to 8 days at −20 °C (n = 30, samples analyzed after 1 or 8 days of storage, t-test). However, Dunham-Cheatham et al.[18] observed that 36 to 46% of permeated $HgBr_2$ was lost from CEM under these storage conditions after 72 days, while ambient Hg^{II} was quantitatively retained after 72 days of storage. Together, these results suggest that permeated $HgBr_2$ may not be stable on the membranes during longer-term storage.

These results indicated that CEM retained ambient Hg^{II}, but lost Hg^{II} permeated from pure solids, over a week of active sampling. It is possible that the permeated Hg^{II} used in this study, loaded over a short period of time (ca. 10 min), was less stable than the ambient Hg^{II} compounds collected during field sampling (i.e., over 7 days). In a previous study, it was reported that CEM collected 30 and 50% less ambient Hg^{II} than codeployed DCS.[13] The DCS was calibrated using $HgBr_2$ from the calibrator. If the permeated $HgBr_2$ was not retained on the CEM and instead measured as GEM, this would bias the GEM measurement high; however, the $HgBr_2$ calibration in the DCS was relatively rapid (e.g., 1 to 3 h) compared to the week-long active sampling of the RMAS, and Hg^{II} losses during this short calibration may be negligible. In addition, the DCS incorporated a heated inlet and sampling line, occasional flushing with zero air (Hg-free) or heated air from its thermal converter, and other features that were different from RMAS membrane deployments, and it is not known whether any of these DCS characteristics led to differences in $HgBr_2$ recovery relative to the RMAS. More work is needed to fully understand the causes for the differences between these measurements.

In field tests, CaP retained the largest amount of the $HgBr_2$ loaded before field deployments (83 ± 15%), similar to codeployed CEM (78 ± 9% for the deployments with metal oxide glasses), followed by significantly less retention by FeP and CaAl (35 ± 17% and 35 ± 22%, respectively; ANOVA) (Figure 3). As quantitatively sorbed Hg^{II} (as $HgBr_2$) in laboratory air was retained, it is likely that constituents in ambient air (e.g., O_3, H_2O) reacted with the loaded $HgBr_2$, leading to release from the surface. Lower retention from FeP and CaAl indicated that the Hg^{II} compounds are more weakly bound compared to the CaP.

https://doi.org/10.1021/acsomega.5c05401
ACS Omega 2025, 10, 47676−47687

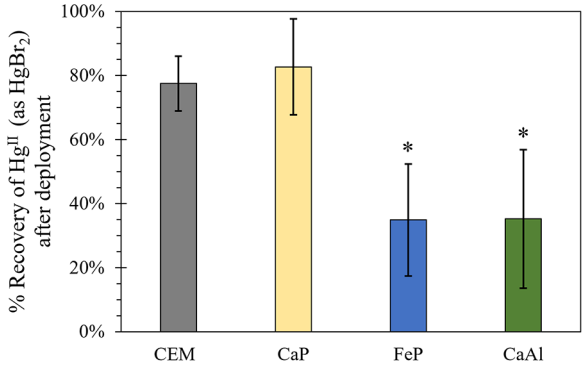

Figure 3. Percent recovery of preloaded Hg^{II} (as $HgBr_2$) following RMAS field deployment from CEM and metal oxides. Error bars represent 1σ (n = 9). * indicates statistical significance relative to the CEM (α = 0.05).

The similar Hg loading behavior observed across the three glasses suggests that their surfaces provide functionally similar surface environments, likely due to terminal hydroxyl sites. Hydroxylation of metal oxide surfaces reduces the electron-donating ability of low-coordinated oxygen sites, thereby decreasing the chemisorption affinity for oxidized Hg species (i.e., direct $O^{2-} \rightarrow Hg^{2+}$ interactions). If the surface is dominated by terminal hydroxyl sites, initial interactions with highly electrophilic $HgBr_2$ likely occur via physisorption (i.e., eq 1) or weak chemisorption involving associative adsorption (i.e., eq 2).[7,35] These weakly surface-bound species are highly susceptible to volatilization or transformation when exposed to humidity, UV, or oxidants like ozone.

$$HgBr_2(g) \leftrightarrow \equiv HgBr_2(ads) \quad (1)$$

$$HgBr_2(g) + \equiv M - OH \leftrightarrow \equiv M - OH\cdots HgBr_2 \quad (2)$$

The unexpected significantly higher retention of Hg^{II} on CaP after exposure to field conditions indicates that there is a fundamental difference in reactions after sorption. TD experiments to 180 °C show the release of Hg from the glassy sorbents with increasing temperature (Figure 4). No Hg nor Br compounds, nor water, were detected with the TGA-MS. It is likely that the masses of sorbed $HgBr_2$ (<1 ng) were below the detection limit of the instrument. Differences in the release of gaseous oxygen with temperature were observed (Figure S9); however, the relationship to structural or chemical changes at the glass surfaces is not clear. XPS analysis indicated that there was no notable variation in the surface oxygen chemical environment among the three glass compositions (Figure S10). As oxygen coordination directly influences surface basicity, these findings suggest that differences in surface reactivity or adsorption behavior across the samples were not likely contributing to variations in oxygen speciation and that basic characteristics across the samples were comparable. These results suggest that while surface hydroxyl groups, and potentially nonbridging/low-coordinated oxygens, present on all glasses may facilitate initial sorption of $HgBr_2$, retention behavior could be governed by subsequent chemical transformations that depend strongly on glass composition and network chemistry. Based on these results, the following reaction between Hg and CaP glass could be represented by a strongly chemisorbed Hg compound involving ligand exchanges (eq 3).

$$HgBr_2(g) + \equiv P - OH \leftrightarrow \equiv P - O - HgBr + HBr(g) \quad (3)$$

Subsequent reactions may occur to form Hg-phosphate complexes.[36] However, it is important to emphasize that additional experimental and theoretical modeling studies are needed to understand the heterogeneous reaction mechanisms leading to capture, phase formation, and subsequent release or immobilization depending on the environmental conditions.

Comparison of Thermal Desorption Profiles from Nylon Membrane Experiments. TD profiles of all field-deployed nylons varied seasonally (Figures 5 and S11). Nylon membranes loaded with Hg^{II} (as $HgBr_2$) consistently exhibited the same bimodal profile shape as nonloaded field controls (Figure 5, yellow curves); this was true of field deployed nylons both preloaded (solid blue curves) and postloaded (dashed blue curves) with $HgBr_2$. Comparison of these profiles demonstrated that $HgBr_2$ was lost from the membrane during deployment. The bimodal profiles of laboratory controls and membranes deployed in the spring had dominant peaks in the 65−75° C and 135−145 °C ranges. Membranes deployed in the summer demonstrated a strong peak around 80 °C with a prominent right tail. In addition, the profiles are similar to those measured previously in Reno, Nevada (cf. Gustin et

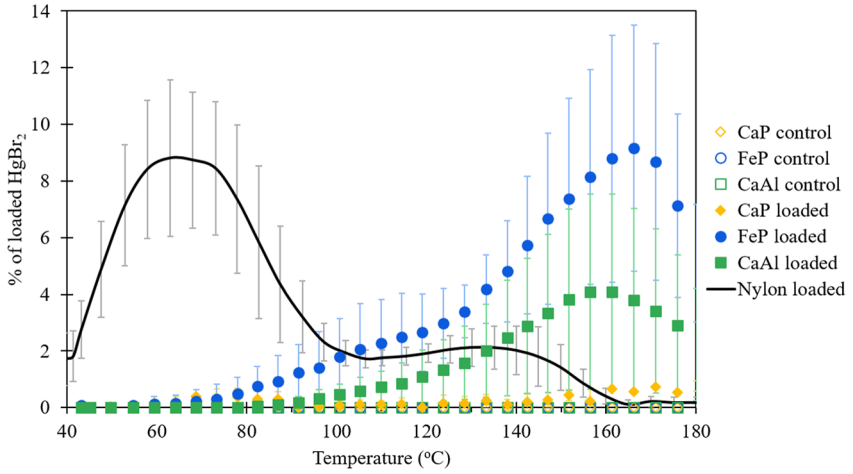

Figure 4. TD results for metal oxide glasses and nylon membranes either not loaded with $HgBr_2$ ("control") or loaded with $HgBr_2$ ("loaded"). Error bars represent 1σ (n = 3 for metal oxide glasses, and 8 for nylon membranes).

https://doi.org/10.1021/acsomega.5c05401
ACS Omega 2025, 10, 47676−47687

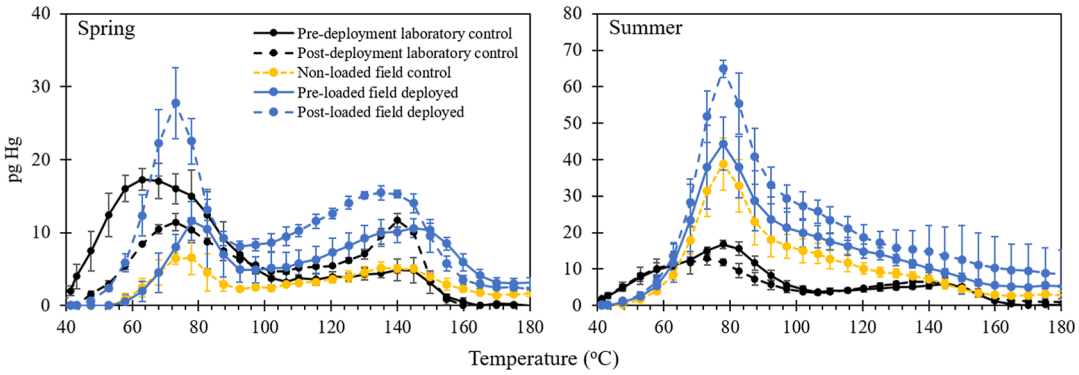

Figure 5. Examples of TD profiles of Sartorius nylons deployed in the RMAS in the field for 1 week during the spring (left) and summer (right) without PTFE. Nondeployed $HgBr_2$-loaded membranes loaded pre- and postdeployment (laboratory controls) are shown in black, nonloaded, deployed field controls are shown as dotted yellow lines, and deployed $HgBr_2$-loaded membranes are shown in blue. Membranes loaded before deployment ("pre-deployment field deployed") are shown with solid lines and membranes loaded after deployment ("post-deployment field deployed") are shown with dashed lines. Error bars represent 1σ (n = 3).

al.[37]), with halogenated compounds being more dominant in the summer along with a variety of compounds (i.e., −O, -Br/Cl, −N, and −S based compounds) depending on the prevailing wind direction. The loaded membranes had significantly more Hg^{II} than the nonloaded field controls (Figures 5, S12−S13, S16), as expected. However, it can be assumed that the loaded field-deployed membranes should have a TD profile more similar to the nonloaded field control plus the corresponding nondeployed laboratory control. When compared to the combined profile of the nonloaded field control and the corresponding laboratory control, the loaded membranes were not significantly different for the peak between 115 and 165 °C, but were significantly different for the peak between 40 and 110 °C (Figures S14−S16), where the TD peak for $HgBr_2$ has been previously reported (see discussion below). The preloaded membranes were significantly lower and the postloaded membranes significantly higher than the combined control TD profiles. These results indicate that some of the $HgBr_2$ loaded on the nylon membranes before deployment was lost from the membrane during deployment. It should be noted that variation in the $HgBr_2$ laboratory control TD profiles existed throughout the seven-month long experiment (Figure S12); in some cases, the differences between the pre- and postdeployment laboratory controls are similar to the differences between the pre- and postloaded field deployed membranes. Based on this variation, the differences between the loaded field-deployed membranes and the combined control TD profiles may not be as significantly different as they otherwise appear. More work is needed to better understand the source of variation in the $HgBr_2$ TD profiles.

The TD profiles of nylon membranes loaded with $HgBr_2$ in this study did not show changes in shape for up to 2 weeks of storage (Figure 6). The profiles were dominated by two peaks, with maxima in the 65 to 70 °C and 135 to 145 °C ranges. Though there were shifts in both peaks through 14 days of storage, these shifts were not significantly different than the immediately analyzed sample (e.g., the regression slopes are not significantly different from 1) (Figure S17). These results indicate that the $HgBr_2$-loaded nylon membranes are stable when stored frozen for at least 14 days. However, the downward shift in the first peak height coupled with the upward shift in the second peak height could indicate that the Hg^{II} compound may be transforming on the nylon membrane

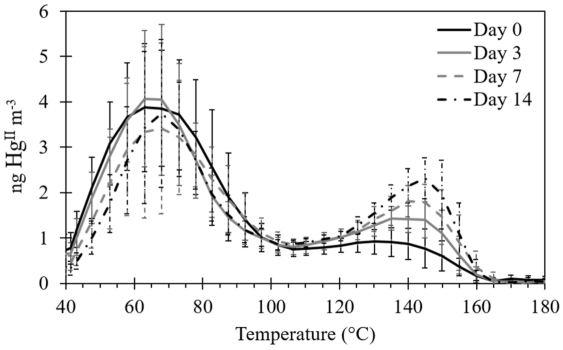

Figure 6. TD profiles of Sartorius nylon membranes loaded with Hg^{II} (as $HgBr_2$) and desorbed 0, 3, 7, or 14 days after loading. Each curve represents the mean of replicate (n = 9) samples. Error bars represent 1σ (n = 9).

surface during storage, leading to slightly different thermal desorption behavior through time. This will require further investigation.

These TD profiles (Figure 6) are the first description of peaks occurring as low as 65 °C. Dunham-Cheatham et al.[18] also observed bimodal peaks at 80 and 145 °C. Profiles developed by Huang et al.[15] had a peak for $HgBr_2$ at 115 °C. This was later adjusted by a negative shift of 15 °C to the 90 to 110 °C range, with the peak maxima at 100 °C, after developing a more efficient thermolyzer and direct temperature measurements within the tube furnace (Luippold et al.[17]). The profile for $HgBr_2$ developed by Huang et al.[15] was comparable to the one developed using direct pyrolysis of the same compound,[38] that also exhibited a bimodal profile.

Differences in the $HgBr_2$ TD profiles presented in these studies may result from small differences between the experiments. $HgBr_2$ in this study was loaded directly into membranes through PFA filter packs drawing laboratory air, a condition that more closely represents atmospheric Hg^{II} sampling in the RMAS compared to the conditions under which standard profiles were developed by Huang et al.[15] Standard profiles in Huang et al.[15] were developed by exposing nylon membranes to Hg^{II} permeated through an uncoated glass manifold in activated carbon (AC)-scrubbed laboratory air with 9 to 20% relative humidity. It is noteworthy that bimodal profiles with peaks at ∼70 and 150 °C were also observed on nylons loaded with $HgBr_2$ or $HgCl_2$ in AC-

https://doi.org/10.1021/acsomega.5c05401
ACS Omega 2025, 10, 47676−47687

scrubbed laboratory air by Dunham-Cheatham et al.[18] Thus, differences in profile shape are likely not due to the use of AC-scrubbed air.

Another potential explanation for the different profiles could be differing atmospheric conditions under which the membranes were loaded with Hg^{II}. In this study, a calibrator was used to transmit volatilized $HgBr_2$ from a permeation tube that contained solid $HgBr_2$ (American Elements) in helium carrier gas diluted with AC-scrubbed laboratory air. In other studies, volatilized $HgBr_2$ was carried from permeation tubes held in a temperature-controlled bath (0 to 10 °C) to the membrane in scrubbed air.[15,18]

Additionally, differences in TD profiles may arise due to differences in the nylon membrane itself, as suggested by Dunham-Cheatham et al.[18] TD profiles of $HgBr_2$ desorbed from Sterlitech and Whatman nylon membranes (Figure 7)

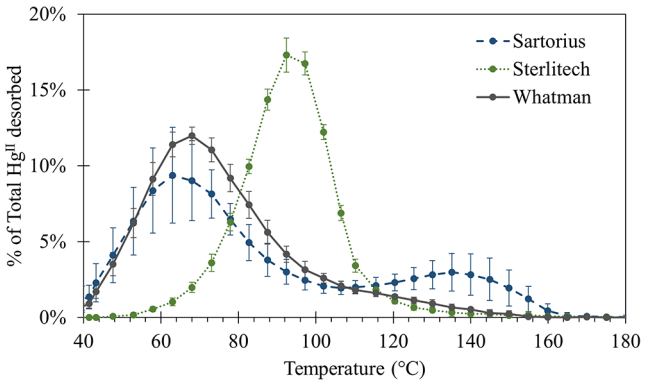

Figure 7. TD profiles of Hg^{II} (loaded as $HgBr_2$) desorbed from Sartorius, Sterlitech, and Whatman nylon membranes. Data points are displayed at each temperature as a % of the total Hg desorbed from each membrane. Error bars represent 1σ (n = 9).

had unimodal profiles, with peak maxima at 95 and 75 °C, respectively, while the Sartorius nylons demonstrated the bimodal profile described above (peaks at 65−70 °C and 135−145 °C). Blank membranes from each manufacturer did not release any detectable Hg (data not shown). This comparison of TD profiles provides evidence that differences in manufacturing between membrane suppliers may be responsible for the differences observed between the TD profiles of $HgBr_2$ presented here and in Dunham-Cheatham et al.[18] compared to those of Huang et al.[15] and Gustin et al.[16]

FTIR was used to investigate potential chemical structure differences between the nylon membranes from different manufacturers. A weak peak at 937 cm^{-1} was identified in the Sterlitech and Whatman membrane spectra, but was mostly absent in the Sartorius spectra (Figure S18). This peak has been interpreted in the literature to represent crystallinity[39] or transisomerism[40] for nylon. The differences in spectra at this wavenumber indicate a structural difference between nylon membrane products, possibly due to differences in manufacturing processes, and may explain differences in the TD profiles of loaded $HgBr_2$. The Sterlitech TD profile for $HgBr_2$ (Figure 7) more closely resembles the $HgBr_2$ standard profile developed by Huang et al.[15]

This study and Dunham-Cheatham et al.[18] utilized nylon membranes purchased directly from Sartorius, while Huang et al.[15] used nylon membranes purchased from Cole-Parmer. However, both membranes were manufactured by Sartorius, as confirmed by Sartorius's sales team (Sartorius, personal communications), and sold under the same part number; thus, the results from both Sartorius and Cole-Parmer nylon should be the same, as they are the same product. A direct comparison of the two nylon membranes, Sartorius vs Cole-Parmer, following the same $HgBr_2$ loading and RMAS methods described above indicated that the membranes do not always capture Hg similarly (Figure S19), despite the materials being the same product and manufactured within 4 months of each other. The differences in TD profiles observed between Huang et al.[15] and later work (e.g., Dunham-Cheatham et al.,[18] Luippold et al.,[17] and this work) may be due to changes in the manufacturing of Sartorius brand membranes over time. Communications with Sartorius indicated that no manufacturing changes have been made to the production process for the nylon membrane product since 2012, but no information could be provided about changes in manufacturing of their nylon material prior to this date (Sartorius, personal communications).

These findings bring to light some considerations regarding published nylon membrane data. Field studies have produced results that are logical in terms of observed Hg^{II} compounds. Multiple lines of evidence (e.g., HYSPLIT back trajectories, criteria pollutant concentrations, meteorological data, and knowledge of Hg sources and atmospheric composition) support the predicted atmospheric Hg^{II} compounds using TD profiles developed using permeated Hg^{II} compounds (ca. Gustin et al.[25,27,37] and Osterwalder et al.[41]). Thus, previous data are useful for thinking about potential atmospheric Hg^{II} compounds, though they likely vary as a function of environmental setting. This information is a stepping stone toward better understanding atmospheric Hg^{II} compounds and chemical reactions. It is apparent from the experiments herein that permeated $HgBr_2$ is stable on membranes for short durations when stored at −20 °C, but not stable on membranes during week-long active ambient sampling; previous studies have shown, however, that ambient Hg^{II} compounds are stable during long-term storage.[18] When TD profiles were initially developed, membranes were loaded with Hg^{II} compounds in scrubbed air in a reaction chamber with permeation tubes held in a controlled temperature bath,[15] but more recent Hg^{II} TD profile development has been performed using a calibrator. Data presented from the experiments described herein demonstrated that permeated $HgBr_2$ may not represent ambient Hg^{II} compounds well.

CONCLUSIONS

Experiments demonstrated that metal oxide glasses (i.e., CaP, FeP, and CaAl) quantitatively sorb $HgBr_2$ without capture of Hg^0 in a laboratory setting and captured more Hg^{II} per m^2 compared to CEM in both laboratory and field settings; however, the metal oxide glasses did not sorb as much total Hg^{II} as the CEM when not normalized to sorbent surface area. The CaP retained the most preloaded $HgBr_2$ after field deployment. These findings indicate that phosphate-based glasses are promising sorbent preconcentration surfaces for Hg^{II} compounds, and could feasibly be utilized in active air samplers. Deployment of these materials in a geometry with higher surface area (e.g., coated membranes) and/or heating should improve the Hg^{II} capture capacity. Future studies should investigate how compositional and structural drivers influence the heterogeneous reaction mechanisms that lead to

https://doi.org/10.1021/acsomega.5c05401
ACS Omega 2025, 10, 47676−47687

Hg^{II} release or immobilization depending on the atmospheric conditions.

Permeated $HgBr_2$ was lost from all materials during field deployment. Similar recoveries were made on both CEM and CaP, with less retention on FeP and CaAl. Dunham-Cheatham et al.[18] observed quantitative retention and lack of transformation of ambient Hg^{II} compounds on CEM and nylon membranes, but losses and transformations of permeated $HgBr_2$, during storage. However, less ambient Hg^{II} was measured on CEM compared to a DCS,[13] indicating that CEM may lose both ambient Hg^{II} and permeated $HgBr_2$ during active sampling, highlighting the importance of identifying or developing new materials that can be used as preconcentration surfaces for the accurate collection and measurement of ambient Hg^{II} compounds.

The Sartorius brand nylon membranes loaded with $HgBr_2$ before or after ambient air exposure had the similar TD profiles as combined controls in field campaigns. The TD profiles of permeated $HgBr_2$ on field-deployed nylon membranes did not conclusively indicate chemical reactions occurring on the nylon surface, but did show some volatile loss of the loaded $HgBr_2$. The TD profile of $HgBr_2$ was shown to vary by nylon manufacturer, suggesting that differences in manufacturing could result in different TD profiles for atmospheric Hg^{II} compounds, and may explain why the $HgBr_2$ TD profiles observed here and in Dunham-Cheatham et al.[18] were different compared to profiles reported by Huang et al.[15] and Gustin et al.[16] This highlights that future TD analyses should assess field samples using standard profiles developed with the same material used to collect field samples.

Future work with any alternative material should include testing with a range of Hg^{II} compounds and atmospheric variables (e.g., O_3, humidity, etc.) to determine if the material selectively and quantitatively captures and retains these compounds under variable atmospheric compositions. A range of Hg^{II} compounds are expected to exist in the atmosphere based on theoretical calculations,[42,43] and these may behave differently on different materials. Promising materials should then be tailored for use as collection surfaces to be used with developed MS methods.

■ ASSOCIATED CONTENT

Supporting Information

The Supporting Information is available free of charge at https://pubs.acs.org/doi/10.1021/acsomega.5c05401.

Additional experimental details, materials, methods, and results (PDF)

■ AUTHOR INFORMATION

Corresponding Author

Sarrah M. Dunham-Cheatham − *College of Agriculture, Biotechnology and Natural Resources, University of Nevada, Reno, Nevada 89557, United States;* orcid.org/0000-0002-2281-1686; Email: sarrahdc@unr.edu

Authors

Livia Lown − *Department of Natural Resources and Environmental Science, University of Nevada, Reno, Nevada 89557, United States*

Paige Murray − *Department of Chemical and Materials Engineering, University of Nevada, Reno, Nevada 89557, United States*

Seth N. Lyman − *Bingham Research Center, Utah State University, Vernal, Utah 89557, United States; Department of Chemistry and Biochemistry, Utah State University, Logan, Utah 89557, United States;* orcid.org/0000-0001-8493-9522

Krista L. Carlson − *Department of Chemical and Materials Engineering, University of Nevada, Reno, Nevada 89557, United States;* orcid.org/0000-0002-4288-2641

Mae Sexauer Gustin − *Department of Natural Resources and Environmental Science, University of Nevada, Reno, Nevada 89557, United States*

Complete contact information is available at: https://pubs.acs.org/10.1021/acsomega.5c05401

Author Contributions

LL designed and executed the experiments, performed data analysis and interpretation, and prepared the manuscript. SMDC helped design the experiments, supervised the experiments and data analysis, and edited the manuscript. SL built and consulted on the use of the $HgBr_2$ calibrator, consulted on experiments, and edited the manuscript. PM made CaP, FeP, and CaAl, and performed the material characterizations. KC suggested the glass compositions and consulted on data interpretation. PM and KC prepared sections discussing glass properties. MSG conceived the project, acquired funding, supervised experiments, and edited the manuscript.

Funding

This work was funded by the National Science Foundation, Division of Atmospheric and Geospace Sciences, under grants 2043042, 2044537, and 1951513. Research conducted by the Carlson lab was supported by the United States Department of Energy (DOE) WTP project office in the Hanford Field Office managed by Albert Kruger under contract 89304021CEM000014 and the US Nuclear Regulatory Commission (USNRC) under contract 31310022M015.

Notes

The authors declare the following competing financial interest(s): The authors declare that the research was conducted in the absence of any commercial or financial relationships that could be construed as a potential conflict of interest. Livia Lown, Sarrah Dunham-Cheatham, Paige Murray, Krista Carlson, and Mae Gustin have a patent pending for application of the metal oxide glass sorbents for Hg^{II} capture.

■ ACKNOWLEDGMENTS

Thanks to Mitch Aiken, Nicole Choma, Abi Connoly, Chris Ford, Sydney McDonald, Ryan Murphy, Momiji Ohyama, Elizabeth Siewert, and Morgan Yeager for help maintaining the trace-clean glassware and equipment used in this study. Thanks to Dr. Monica Arienzo at Desert Research Institute for providing FTIR spectra for the nylon membranes. And thank you to 4 anonymous reviewers for their thoughtful feedback.

■ REFERENCES

(1) Deeds, D. A.; Ghoshdastidar, A.; Raofie, F.; Guérette, E. A.; Tessier, A.; Ariya, P. A. Development of a particle-trap preconcentration-soft ionization mass spectrometric technique for the quantification of mercury halides in air. *Anal. Chem.* **2015**, *87* (10), 5109−5116.

(2) Jones, C. P.; Lyman, S. N.; Jaffe, D. A.; Allen, T.; O'Neil, T. L. Detection and quantification of gas-phase oxidized mercury compounds by GC/MS. *Atmos. Meas. Tech* **2016**, *9* (5), 2195−2205.

(3) Khalizov, A. F.; Guzman, F. J.; Cooper, M.; Mao, N.; Antley, J.; Bozzelli, J. Direct detection of gas-phase mercuric chloride by ion drift-chemical ionization mass spectrometry. *Atmos. Environ.* **2020**, *238*, 117687.
(4) Mao, N.; Khalizov, A. Exchange reactions alter molecular speciation of gaseous oxidized mercury. *ACS Earth Space Chem.* **2021**, *5* (8), 1842−1853.
(5) Gustin, M. S.; Dunham-Cheatham, S. M.; Huang, J.; Lindberg, S.; Lyman, S. N. Development of an understanding of reactive mercury in ambient air: A review. *Atmosphere* **2021**, *12* (1), 73.
(6) Tang, H.; Li, C.; Duan, Y.; Zhu, C.; Cai, L. Combined experimental and theoretical studies on adsorption mechanisms of gaseous mercury (II) by calcium-based sorbents: The effect of unsaturated oxygen sites. *Sci. Total Environ.* **2019**, *656*, 937−945.
(7) Urba, A.; Valiulis, D.; Šarlauskas, J.; Kvietkus, K.; Šakalys, J.; Selskis, A. A pilot study of different materials applied for active sampling of gaseous oxidized mercury in the atmospheric air. *Atmos. Pollut. Res.* **2017**, *8* (4), 791−799.
(8) Wang, F.; Wang, S.; Meng, Y.; Zhang, L.; Wu, Q.; Hao, J. Mechanisms and roles of fly ash compositions on the adsorption and oxidation of mercury in flue gas from coal combustion. *Fuel* **2016**, *163*, 232−239.
(9) Zheng, Y.; Duan, Y.; Tang, H.; Li, C.; Li, J.; Zhu, C.; et al. Experimental research on selective adsorption of gaseous mercury (II) over SiO2, TiO2 and γ-Al2O3. *Fuel* **2019**, *237*, 202−208.
(10) Tang, H.; Duan, Y.; Zhu, C.; Cai, T.; Li, C.; Cai, L. Theoretical evaluation on selective adsorption characteristics of alkali metal-based sorbents for gaseous oxidized mercury. *Chemosphere* **2017**, *184*, 711−719.
(11) Shen, A.; Liu, X.; Li, H.; Duan, Y. DFT study of mercury adsorption on Al2O3 with presence of HCl. *J Mol Graph Model.* **2023**, *124*, 108548.
(12) Jampaiah, D.; Ippolito, S. J.; Sabri, Y. M.; Tardio, J.; Selvakannan, P. R.; Nafady, A.; Reddy, B. M.; Bhargava, S. K. Ceria-zirconia modified MnOx catalysts for gaseous elemental mercury oxidation and adsorption. *Catal. Sci. Technol.* **2016**, *6*, 1792.
(13) Dunham-Cheatham, S. M.; Lyman, S.; Gustin, M. S. Comparison and calibration of methods for ambient reactive mercury quantification. *Sci. Total Environ.* **2023**, *856*, 159219.
(14) Allen, N.; Gačnik, J.; Dunham-Cheatham, S. M.; Gustin, M. S. Interaction of reactive mercury with surfaces and implications for atmospheric mercury speciation measurements. *Atmos. Environ.* **2024**, *318*, 120240.
(15) Huang, J.; Miller, M. B.; Weiss-Penzias, P.; Gustin, M. S. Comparison of gaseous oxidized Hg measured by KCl-coated denuders, and nylon and cation exchange membranes. *Environ. Sci. Technol.* **2013**, *47* (13), 7307−7316.
(16) Sexauer Gustin, M.; Pierce, A. M.; Huang, J.; Miller, M. B.; Holmes, H. A.; Loria-Salazar, S. M. Evidence for different reactive Hg sources and chemical compounds at adjacent valley and high elevation locations. *Environ. Sci. Technol.* **2016**, *50*, 12225−12231.
(17) Luippold, A.; Gustin, M. S.; Dunham-Cheatham, S. M.; Zhang, L. Improvement of quantification and identification of atmospheric reactive mercury. *Atmos. Environ.* **2020**, *224*, 117307.
(18) Dunham-Cheatham, S. M.; Lyman, S.; Gustin, M. S. Evaluation of sorption surface materials for reactive mercury compounds. *Atmos. Environ.* **2020**, *242*, 117836.
(19) Howard, J.; Gardner, L.; Saifee, Z.; Geleil, A.; Nelson, I.; Colombo, J. S.; Naleway, S. E.; Carlson, K. Synthesis and characterization of novel calcium phosphate glass-derived cements for vital pulp therapy. *J. Mater. Sci.: Mater. Med.* **2020**, *31*, 12.
(20) Riley, B. J.; Peterson, J. A.; Vienna, J. D.; Ebert, W. L.; Frank, S. M. Dehaloganation of electrochemical processing salt simulants with ammonium phosphates and immobilization of salt cations in an iron phosphate glass waste form. *J. Nucl. Mater.* **2020**, *529*, 151949.
(21) Dumarey, R.; Brown, R. J. C.; Corns, W. T.; Brown, A. S.; Stockwell, P. B. Elemental mercury vapour in air: the origins and validation of the 'Dumarey equation' describing the mass concentration at saturation. *Accredit. Qual. Assur.* **2010**, *15*, 409−414.
(22) Elgiar, T. R.; Lyman, S. N.; Andron, T. D.; Gratz, L.; Hallar, A. G.; Horvat, M.; Vijayakumaran Nair, S.; O'Neil, T.; Volkamer, R.; Živković, I. Traceable Calibration of Atmospheric Oxidized Mercury Measurements. *Environ. Sci. Technol.* **2024**, *58*, 10706−10716.
(23) Gačnik, J.; Lyman, S.; Dunham-Cheatham, S. M.; Gustin, M. S. Limitations and insights regarding atmospheric mercury sampling using gold. *Anal. Chim. Acta* **2024**, *1319*, 342956.
(24) Lown, L.; Dunham-Cheatham, S. M.; Lyman, S. N.; Gustin, M. S. Alternate materials for the capture and quantification of gaseous oxidized mercury in the atmosphere. *Atmos. Meas. Tech* **2024**, *17*, 6397−6413.
(25) Gustin, M. S.; Dunham-Cheatham, S. M.; Allen, N.; Choma, N.; Johnson, W.; Lopez, S.; et al. Observations of the chemistry and concentrations of reactive Hg at locations with different ambient air chemistry. *Sci. Total Environ.* **2023**, *904*, 166184.
(26) Luippold, A.; Gustin, M. S.; Dunham-Cheatham, S. M.; Castro, M.; Luke, W.; Lyman, S.; et al. Use of multiple lines of evidence to understand reactive mercury concentrations and chemistry in Hawai'i, Nevada, Maryland, and Utah, USA. *Environ. Sci. Technol.* **2020**, *54* (13), 7922−7931.
(27) Gustin, M. S.; Dunham-Cheatham, S. M.; Zhang, L.; Lyman, S.; Choma, N.; Castro, M. Use of membranes and detailed HYSPLIT analyses to understand atmospheric particulate, gaseous oxidized, and reactive mercury chemistry. *Environ. Sci. Technol.* **2021**, *55* (2), 893−901.
(28) Gustin, M. S.; Dunham-Cheatham, S. M.; Zhang, L. Comparison of 4 methods for measurement of reactive, gaseous oxidized, and particulate bound mercury. *Environ. Sci. Technol.* **2019**, *53* (24), 14489−14495.
(29) Legendre, P. *lmodel2: Model II Regression*. R package Version 2018, *1*, 7−3.
(30) Brow, R. K. Review: the structure of simple phosphate glasses. *J. Non-Cryst. Solids* **2000**, *263*, 1−28.
(31) Brow, R. K.; Kim, C. W.; Reis, S. T. Iron polyphosphate glasses for waste immobilization. *Int. J. Appl. Glass Sci.* **2020**, *11* (1), 4−14.
(32) Yu, X.; Day, D. E.; Long, G. J.; Brow, R. K. Properties and structure of sodium-iron phosphate glasses. *J. Non-Cryst. Solids* **1997**, *215* (1), 21−31.
(33) Bingham, P. A.; Barney, E. R. Structure of iron phosphate glasses modified by alkali and alkaline earth additions: Neutron and X-ray diffraction studies. *J. Phys.: Condens. Matter* **2012**, *24*, 175403.
(34) Lin, Y.; Smedskjaer, M. M.; Mauro, J. C. Structure, properties, and fabrication of calcium aluminate-based glasses. *Int. J. Appl. Glass Sci.* **2019**, *10* (4), 488−501.
(35) Lyman, S. N.; Jaffe, D. A.; Gustin, M. S. Release of mercury halides from KCl denuders in the presence of ozone. *Atmos. Chem. Phys.* **2010**, *10*, 8197−8204.
(36) Kozin, L. F.; Hansen, S.. *Mercury Handbook: Chemistry, Applications and Environmental Impact*. RSC Publishing.2013
(37) Gustin, M. S.; Dunham-Cheatham, S. M.; Choma, N.; Shoemaker, K.; Allen, N. Determining sources of reactive mercury compounds in Reno, Nevada, United States. *Front. Environ. Chem.* **2023**, *4*, 1202957.
(38) Rumayor, M.; Diaz-Somoano, M.; Lopez-Anton, M. A.; Martinez-Tarazona, M. R. Mercury compounds characterization by thermal desorption. *Talanta* **2013**, *114*, 318−322.
(39) Galimberti, D.; Quarti, C.; Milani, A.; Brambilla, L.; Civalleri, B.; Castiglioni, C. IR spectroscopy of crystalline polymers from ab initio calculations: Nylon 6, 6. *Vib. Spectrosc.* **2013**, *66*, 83−92.
(40) Quintanilla, L.; Rodriguez-Cabello, J. C.; Pastor, J. M. Structural analysis of injection-moulded semicrystalline polymers by Fourier-transform infra-red spectroscopy with photoacoustic detection and differential scanning calorimetry: 2. Polyamide-6, 6. *Polymer* **1994**, *35* (11), 2321−2328.
(41) Osterwalder, S.; Dunham-Cheatham, S. M.; Ferreira Araujo, B.; et al. Fate of springtime atmospheric reactive mercury: Concentrations and deposition at Zeppelin, Svalbard. *ACS Earth Space Chem.* **2021**, *5* (11), 3234.

https://doi.org/10.1021/acsomega.5c05401
ACS Omega 2025, 10, 47676−47687

(42) Jiao, Y.; Dibble, T. S. Structures, vibrational frequencies, and bond energies of the BrHgOX and BrHgXO species formed in atmospheric mercury depletion events. *J. Phys. Chem. A* **2017**, *121* (41), 7976−7985.
(43) Shah, V.; Jacob, D. J.; Thackray, C. P.; Wang, X.; Sunderland, E. M.; Dibble, T. S.; et al. Improved mechanistic model of the atmospheric redox chemistry of mercury. *Environ. Sci. Technol.* **2021**, *55* (21), 14445−14456.

https://doi.org/10.1021/acsomega.5c05401
ACS Omega 2025, 10, 47676−47687